IOSR Journal of Pharmacy and Biological Sciences (IOSR-JPBS)
e-ISSN:2278-3008, p-ISSN:2319-7676. Volume 20, Issue 3 Ser. 4 (May. – June. 2025), PP 53-69
www.iosrjournals.org

Identification of novel anticancer agents of Quinoline Containing Chromene Based 1,2,3-Triazoles in their molecular docking studies

Balaswamy. Aleti[a], Kishan. Chevula [a], Nagesh. Patnam [a], Prasad. Chennamsetti[a], KamalakerReddy[b], Praveen Kumar. Edigi [b], Sai Prasad Gedam[c],VijjulathaManga[a,]*,

[a]*MolecularModelling and Medicinal Chemistry Lab, Department of Chemistry, Osmania University, Hyderabad-500007, Telangana, India.*
[b]*Departmentof Chemistry, University College of Science, Osmania University, Hyderabad-500007, Telangana,India.*
[c]*Department of Chemistry Government Degree College, Utnoor, Adilabad- 504311, India.*

Abstract
*A novel library of 2-amino-7,7-dimethyl-5-oxo-4-(2-oxo-1-((subtituted-phenyl-1H-1,2,3-triazol-4-yl)methyl)-1,2-dihydroquinolin-3-yl)-5,6,7,8-tetrahydro-4H-chromene-3-carbonitriles(**9a-h**)was developed utilizing 2-chloroquinoline-3-carbaldehydeas precursor, incorporating multicomponent synthesis and click chemistry reactions. The compounds were evaluated for their in vitro anticancer activity against human breast adenocarcinoma (MCF-7) and human hepatoma cell line (HepG-2) with Doxorubicin serving as the standard reference. Notably, the activities of all compounds exhibited greater effectiveness against these cell lines. Compound **9e**, which features a meta-dichlorosubstitution on the phenyl ring, demonstrated remarkable activity against both two cell lines, exhibiting IC_{50} values of 24.45±1.27μM (MCF-7) and 27.27±0.32μM (HepG-2)surpassing those of the reference drug. Furthermore, compound **9g**, possessing a methyl group in the para position of the phenyl ring, exhibited superior activity with IC_{50} values of 25.32±1.19μM and 29.11±0.03μMagainst MCF-7 and HepG-2 cell lines, respectively. Additionally, a molecular docking study conducted against the crystal structure of Enol-ACP Reductase and RdRp OF HCV (NS5B) revealed favorable binding interactions, corroborating the experimental findings.*

Key words: *1,2,3-triazole, quinoline,chromene, anticancer activity and molecular docking.*

Date of Submission: 25-06-2025 Date of Acceptance: 05-07-2025

I. Introduction:

Cancer remains one of the most significant diseases globally [1]. Following a comprehensive analysis of various diseases, cancer has been identified as the second leading cause of mortality, trailing only cardiac arrest [2]. The most commonly diagnosed types of cancer are breast cancer in women and lung cancer in men, followed by liver cancer and colorectal cancer [3]. Distinct forms of cancer arise from alterations or abnormalities in the typically functioning genetic material [4]. A prevalent strategy to combat the unregulated proliferation, metastasis, and cell division of cancer cells involve the use of medications that disrupt the synthesis and normal function of nucleic acids, namely DNA and RNA [5,6].In recent decades, significant progress has been made in the quest for chemotherapeutic agents as anticancer treatments. However, these chemical agents often result in severe side effects characterized by off-target toxicity and drug resistance. Global expenditure on cancer therapeutics continues to escalate markedly, encompassing both therapeutic and supportive care [7]. Therefore, there exists an urgent need to discover new cancer drugs that leverage the distinctive properties of cancer cells to achieve enhanced inhibitory efficacy without adversely affecting normal cells, thereby necessitating the exploration of novel agents that exhibit low side effects and high efficiency [8].

The EGFR pathway has proven to be crucial in cancer therapy, as unique EGFR signaling constitutes a prominent characteristic of numerous human malignancies [9]. Gefitinib, dacomitinib,afatinibosimertinib, and erlotinib are the initial EGFR-TKIs that received approval from the FDA for the treatment of non-small-cell lung cancer. Subsequently, erlotinib, lapatinib, and icotinib were authorized by the FDA as first-line therapies for pancreatic cancer due to their reversible binding to the EGFR [10]. Research indicates that co-augmentation of EGFR and HER2 occurs in various tumors, including breast, ovarian, prostate, and colorectal cancers, among

others [11]. In the case of breast cancer, the co-overexpression of EGFR and HER2 may result in a poor prognosis and drug resistance. Consequently, targeting solely HER2 may not be adequate for effective treatment. The interactions among HER2 family members and their collaborative functions suggest that a dual-targeting approach, addressing both HER2 and EGFR simultaneously, is a rational strategy [12].

The 1,2,3-triazole nitrogen-rich heterocyclic scaffolds are regarded as amide bioisosteres, capable of forming a variety of non-covalent interactions such as vander Waals forces and hydrogen bonds with numerous proteins, enzymes, and receptors [13]. Their high resistance to enzymatic degradation enhances their potential application in medicinal chemistry. Recently, there has been a notable increase in the utilization of these heterocyclic compounds in various therapeutic areas, including anti-oxidant [14], anti-malarial [15], anti-microbial [16], anti-epileptic [17], anti-tubercular [18], anti-viral [19], anti-diabetic [20], anti-cancer [21, 22], and anti-allergic [23] applications. The 1,2,3-triazole core also serves as an excellent scaffold for the discovery of potent anticancer agents, with compounds such as Cefatrizine and 1,2,3-triazole-dithiocarbamate having already been utilized against human cancer cell lines, including those from colon, lung, prostate, and breast cancers [24, 25].In addition, it is widely recognized that the most significant aspect of the activity of 4-Aryl-4H chromenes lies in their ability to modulate apoptosis through cell- and caspase-based protocols targeting cancer cells, resulting in growth inhibition and ultimately cell death [26]. 4-aryl-4H chromenes act as potent inducers of apoptosis via tubulin inhibition, thus highlighting the critical role of the 4-position in the structure-activity relationship of these derivatives by influencing their apoptotic modulation effects on cancer cells [27]. These scaffolds may be evolved into new therapeutic anticancer regimes because they are also very successful in treating drug-resistant cancer cell lines, either alone or in combination with other anticancer treatments in a variety of tumor models [28-30].

As part of our attempts to create new functional molecules with anticancer potential,we have designed and synthesized a range of functional 4H-chromene derivatives, that include anticancer pharmacophore moieties on the 1,2,3-triazolyl core.

II. Result and discussion

Chemistry

The synthesis title compounds 2-amino-7,7-dimethyl-5-oxo-4-(2-oxo-1-((subtituted-phenyl-1H-1,2,3-triazol-4-yl)methyl)-1,2-dihydroquinolin-3-yl)-5,6,7,8-tetrahydro-4H-chromene-3-carbonitrile(**9a-h**) is summarized in scheme1. The synthesis started with 2-chloroquinoline-3-carbaldehyde (1) was refluxed in 70% acetic acid for 6 hrs to obtain 2-hydroxyquinoline-3-carbaldehyde(2) wasallowed to react with propargyl bromide(3) in DMF using K_2CO_3at rtfor 4hrs to yielded 2-oxo-1-(prop-2-yn-1-yl)-1,2-dihydroquinoline-3-carbaldehyde(4).The compound (4) was reacted with 5,5-dimethylcyclohexane-1,3-dione(5), Malononitrile(6) inpresence of ethanol and catalytical amount of piperzine rt for 1 hr to yielded of cyclization products of 2-amino-7,7-dimethyl-5-oxo-4-(2-oxo-1-(prop-2-yn-1-yl)-1,2-dihydroquinolin-3-yl)-5,6,7,8-tetrahydro-4H-chromene-3-carbonitrile(7). The intermediate compound of terminal alkyne compound (7) on further reaction with various substituted aryl azides(**8a-h**) in click reactionresulted respective2-amino-7,7-dimethyl-5-oxo-4-(2-oxo-1-((subtituted-phenyl-1H-1,2,3-triazol-4-yl)methyl)-1,2-dihydroquinolin-3-yl)-5,6,7,8-tetrahydro-4H-chromene-3-carbonitrile(**9a-h**), the products were obtained in good yields.

Anticancer activity:

The novel hybrid molecules (9a-h) were screened for their in vitro anticancer activity against two human cancer cell lines MCF-7 and HepG-2 using doxorubicin as a standard drug. Table 1 shows the calculated IC_{50} values of all the compounds The compounds meta-dichloro**9d,** para-methyl **9f**, para-methoxy **9g** and para-chloro**9e**showed superior activity against both MCF-7 and HepG-2 cells with IC_{50} of **24.45±1.27**, **27.27±0.32, 25.32±1.19**, **29.11±0.03, 28.35±1.32, 32.54±0.19**and **33.31±1.26, 37.43±0.82µM**, respectively than the standard drug doxorubicin. The observed activity of compound 9d, 9f, 9g and 9d may be attributed to electron electron donating and with drawing effect of meta-dichloro, para-methyl, para-methoxy, and para-chlorogroups are ortho and para directing nature which activates triazole ring. The other compounds substituted with withdrawing group indicated good to poor activity.

Table1. Anticancer activity of the synthesized compounds (9a-h).

Compound Code	MCF-7	HepG-2
9a	41.32±1.31	45.67±0.09
9b	56.79±1.67	59.98±0.18
9c	37.76±1.57	39.43±0.34
9d	**24.45±1.27**	**27.27±0.32**
9e	33.31±1.26	37.43±0.82
9f	**25.32±1.19**	**29.11±0.03**
9g	**28.35±1.32**	**32.54±0.19**
9h	40.38±1.56	52.21±0.90
Doxorubicin	**24.32± 1.09**	**27.57±0.33**

Docking studies against Enol reductase:

Molecular docking investigations were performed on the novel derivatives **(9a-h)** along with the standard drug doxorubicin, and widely used drug Tamoxifen. It is a selective estrogen receptor modulator (SERM) commonly used in the treatment and prevention of breast cancer[31]against the Enoyl reductase(PDB ID: 1QSG)[32], Enoyl-ACP reductase, a critical enzyme in the fatty acid synthesis pathway, is vital for lipid biosynthesis, which supports the rapid growth and proliferation of cancer cells. Over expression of this enzyme is common in various cancers, such as breast, prostate, and lung cancers [33], and is associated with tumor aggressiveness and poor prognosis. Targeting enoyl-ACP reductase with specific inhibitors can disrupt cancer cell metabolism by limiting the availability of essential fatty acids, thus inhibiting tumor growth and promoting apoptosis [34]. This makes enoyl-ACP reductase a promising therapeutic target in the development of novel anti-cancer agents.

All the compounds **(9a-h)** displayed binding energies ranging from -9.8 Kcal/mol to -12 kcal/mol, which is superior to the binding energy of the standard doxorubicin (-8.5 KCal/mol) and tamoxifen (-8.4 KCal/mol).The results are tabulated in **Table-1**.Notably, compounds 9e, 9g, and 9i scored binding energies of -12, -11.8, and -11.3 Kcal/mol respectively, displaying their superior binding affinities. This can be attributed to the conventional hydrogen bonding interactions, carbon-hydrogen bonding, pi-sigma, pi-anion, pi-cation, pi-alkyl, and Vanderwaals interactions between the novel compounds and the Enoyl reductase.

Table-1: Binding affinities of synthesized compounds and interacting amino acids

Molecule	B.E	Interacting A.A Residues	
		H-Bonding	Other types of Interactions
9a	**-10.7**	SER 91, LEU 144, LYS 163	GLY 13, ALA 15, SER 19, ILE 20, HIS 90, ILE 92, GLY 93, PHE 94, ALA 95, LEU 100, SER 145, TYR 146, TYR 156, MET 159, PRO 191, ILE 192, ALA 196, ALA 197, GLY 199, ILE 200, PHE 203,
9b	**-9.9**	GLY 93	GLY 13, ALA 15, SER 19, ILE 20, GLN 40, LEU 44, SER 91, ILE 92, PHE 94, TYR 146, TYR 156, MET 159, LYS 163, PRO 191, THR 194, LEU 195, ALA 196, ALA 197, ILE 200, PHE 203, MET 206
9c	**-10.2**	SER 145, THR 194	ILE 20, SER 91, GLY 93, PHE 94, ALA 95, GLY 97, LEU 100, LEU 144, TYR 146, TYR 156, MET 159, LYS 163, ILE 187, SER 188, PRO 191, ILE 192, ALA 196, ALA 197, GLY 199, ILE 200, PHE 203, MET 206
9d	**-12.0**	SER 91	THR 12, GLY 13, ALA 15, SER 19, ILE 20, THR 38, TYR 39, GLN 40, CYS 63, ASP 64, VAL 65, ILE 92, GLY 93, ILE 119, LEU 144, SER 145, TYR 146, TYR 156, LYS 163, PRO 191, ILE 192, THR 194, LEU 195, ALA 196, ALA 197, ILE 200, PHE 203
9e	**-10.9**	GLN 40	ALA 15, SER 16, SER 19, ILE 20, ALA 21, LEU 44, SER 91, ILE 92, GLY 93, LEU 100, LEU 144, TYR 146, TYR 156, MET 159, LYS 163, ALA 189, PRO 191, ILE 192, THR 194, LEU 195, ALA 196, ALA 197, ILE 200, PHE 203
9f	**-11.8**	ILE 20, SER 91, GLY 93, SER 145	GLY 13, ALA 15, SER 16, LEU 18, SER 19, ALA 21, GLN 40, LEU 44, ILE 92, GLY 93, LEU 144, TYR 146, TYR 156, MET 159, LYS 163, GLY 190, PRO 191, ILE 192, THR 194, ALA 196, ILE 200, PHE 203, MET 206

9g	**-11.2**	ILE 20, SER 91, GLY 93	ALA 15, SER 16, SER 19, ILE 20, ALA 21, GLN 40, LEU 44, ILE 92, GLY 93, LEU 144, SER 145, TYR 146, TYR 156, MET 159, LYS 163, ALA 189, GLY 190, PRO 191, ILE 192, THR 194, ALA 196, ILE 200, PHE 203, MET 206
9h	**-9.8**	SER 91, LEU 144, LYS 163	GLY 13, ALA 15, SER 19, ILE 20, HIS 90, ILE 92, GLY 93, PHE 94, ALA 95, GLY 97, LEU 100, SER 145, TYR 156, MET 159, PRO 191, ILE 192, ALA 196, ALA 197, GLY 199, ILE 200, PHE 203
Tamoxifen	**-8.4**	NIL	SER 19, ILE 20, ALA 21, SER 91, GLY 93, PHE 94, ALA 95, LEU 100, LEU 144, TYR 146, TYR 156, MET 159, LYS 163, ALA 189, GLY 190, PRO 191, ILE 192, THR 194, ALA 196, ALA 197, GLY 199, ILE 200, PHE 203, MET 206
doxo	**-8.5**	ILE 20, GLY 93, LEU 195	GLY 13, VAL 14, ALA 15, SER 16, SER 19, ALA 21, GLN 40, LEU 44, CYS 63, ASP 64, VAL 65, SER 91, ILE 92, PHE 94, ILE 119, LEU 144, LYS 163, THR 194, ALA 196

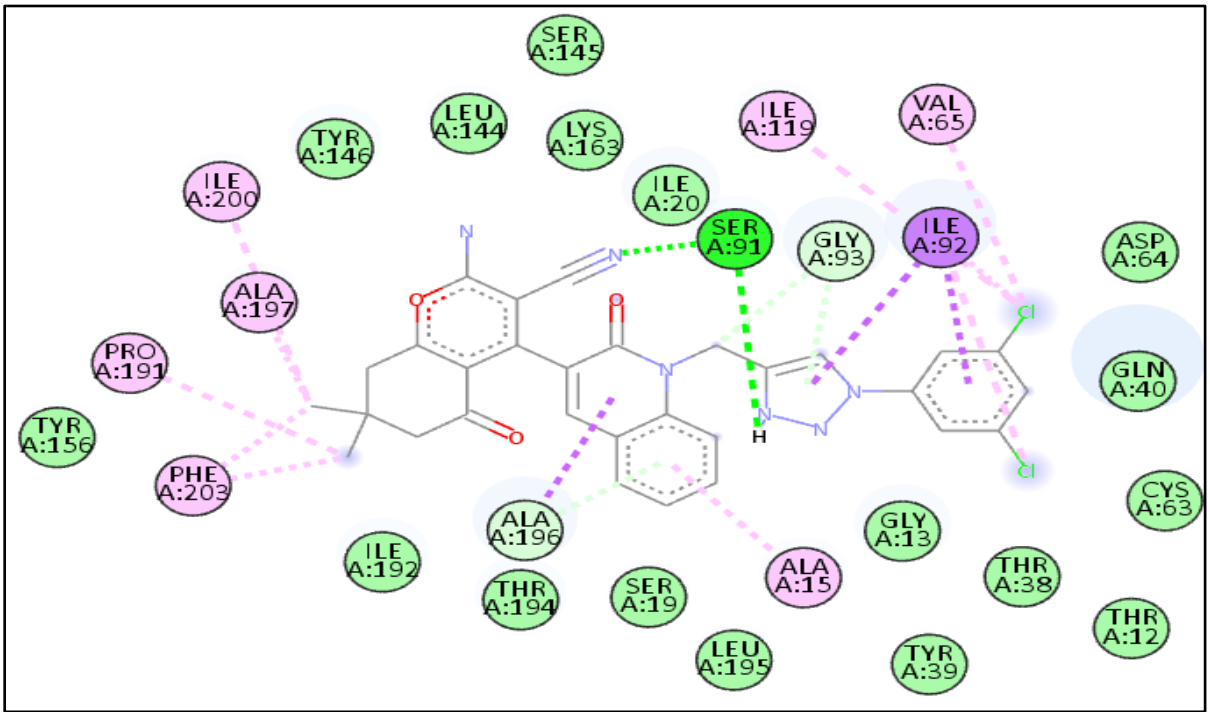

Fig 1:2D Interaction image of '9d' with the Enoyl Reductase

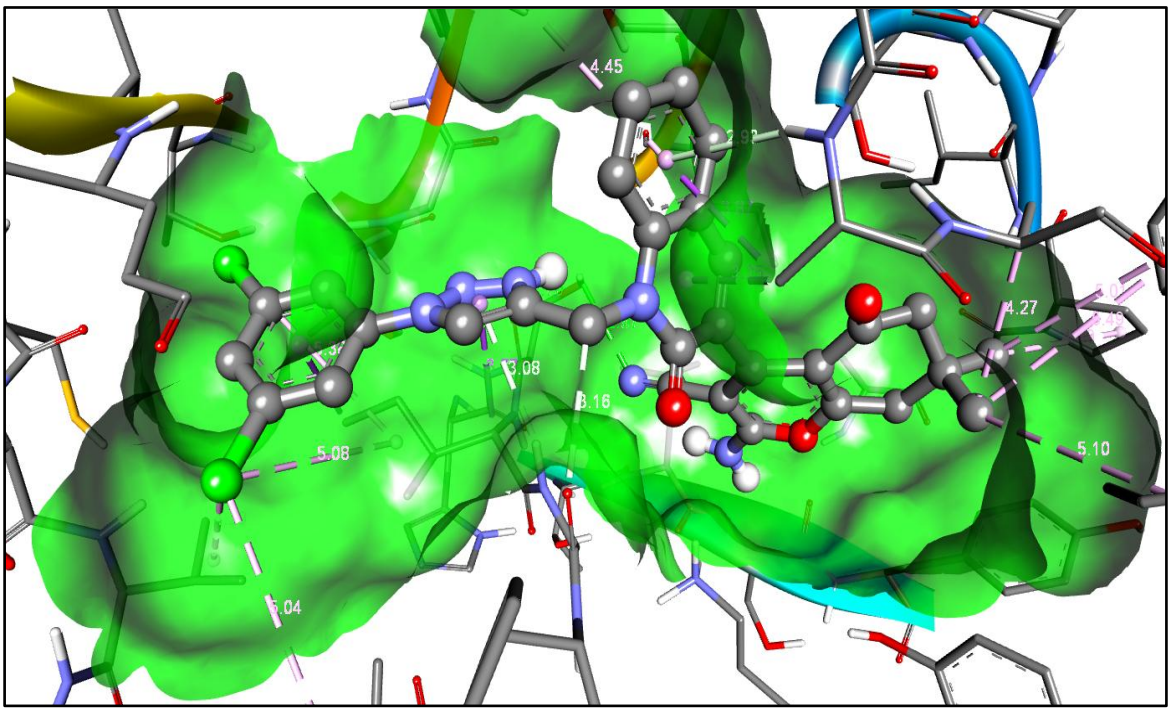

Fig 2:3D Interaction image of '9d' with the Enoyl Reductase

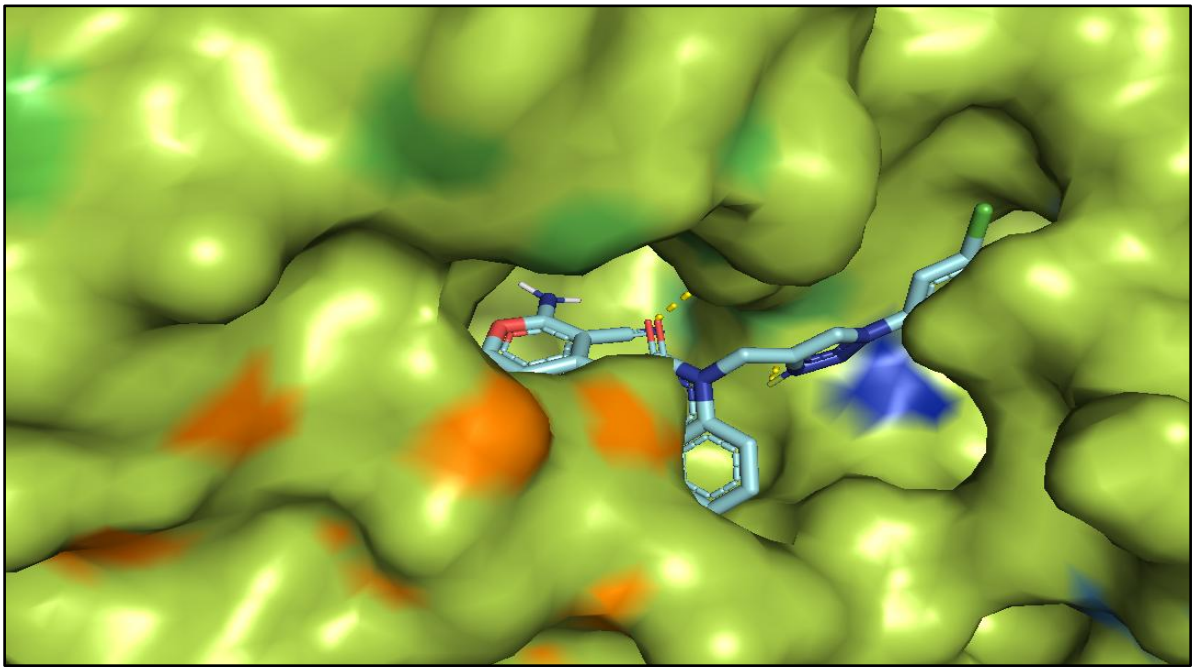

Fig 3:'9d' in the binding pocket of Enoyl Reductase

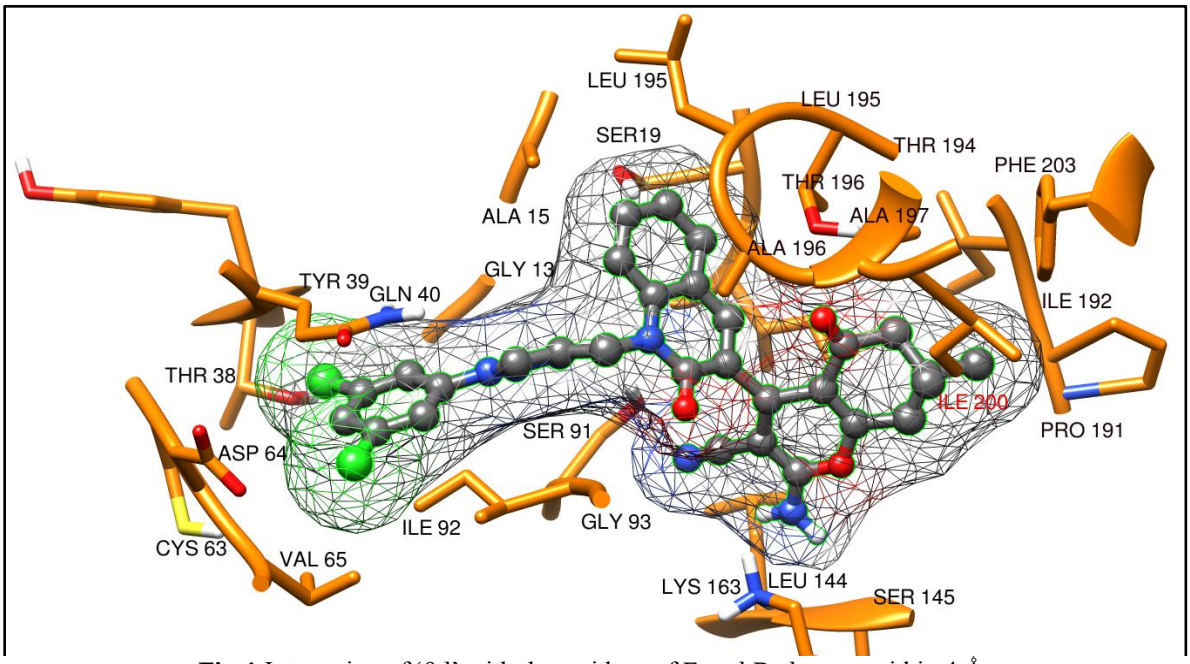

Fig 4: Interaction of '9d' with the residues of Enoyl Reductase within 4 Å

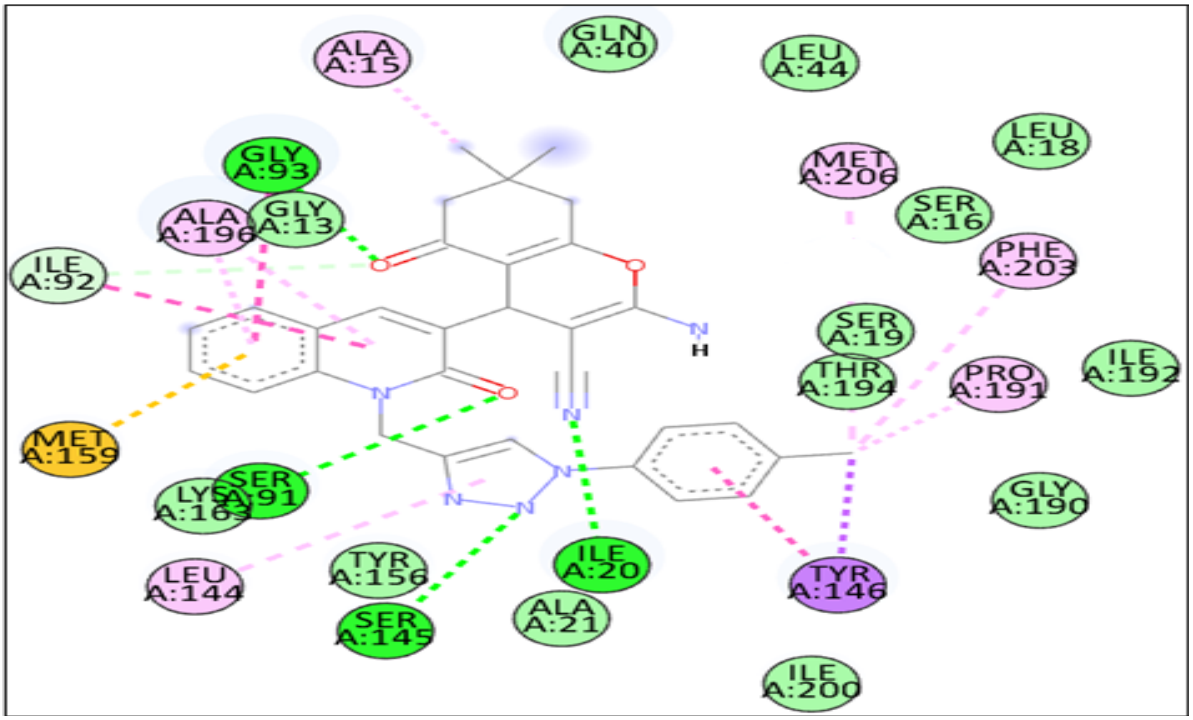

Fig 5:2D Interaction image of '9f' with the Enoyl Reductase

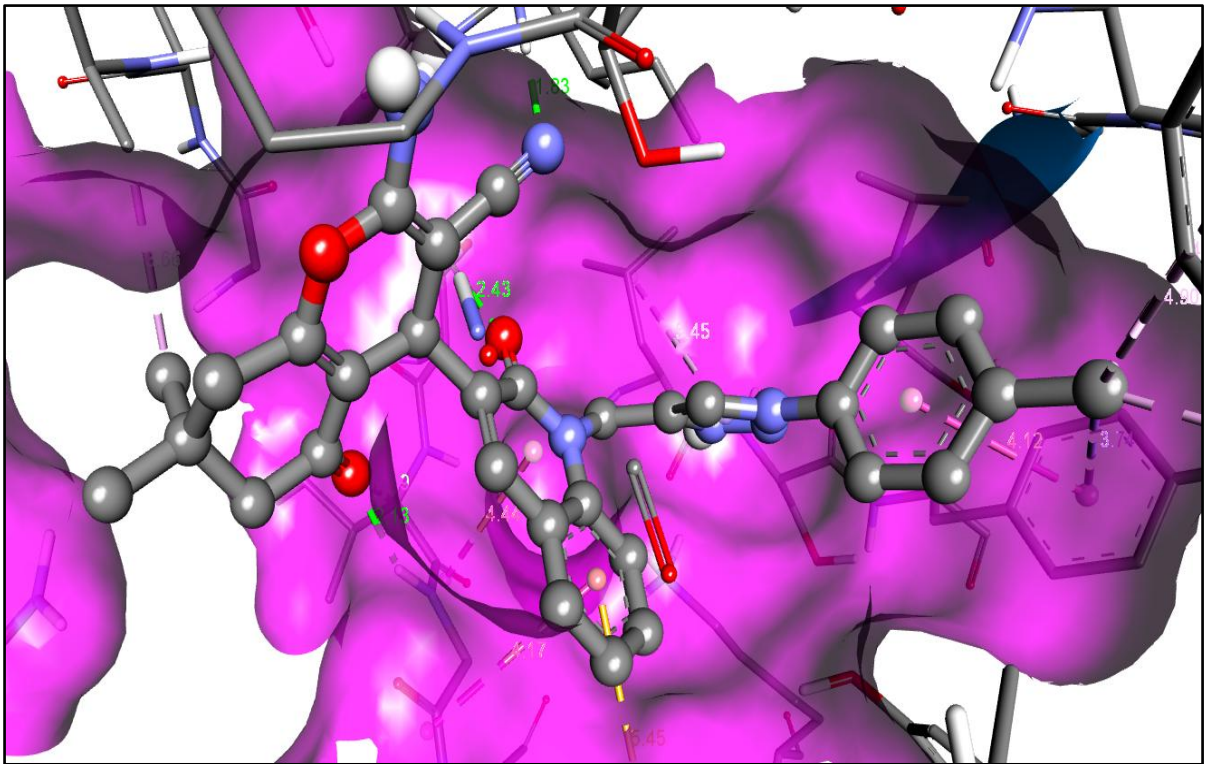

Fig 6:3D Interaction image of '9f' with the Enoyl Reductase

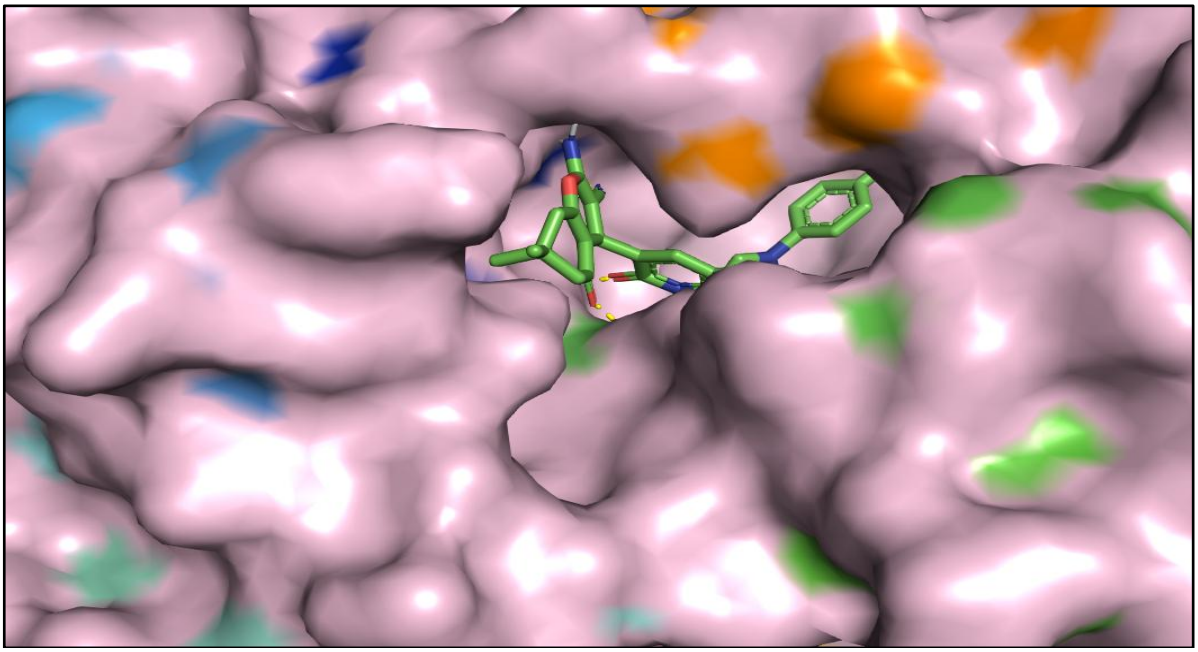

Fig 7:'9f' in the binding pocket of Enoyl Reductase

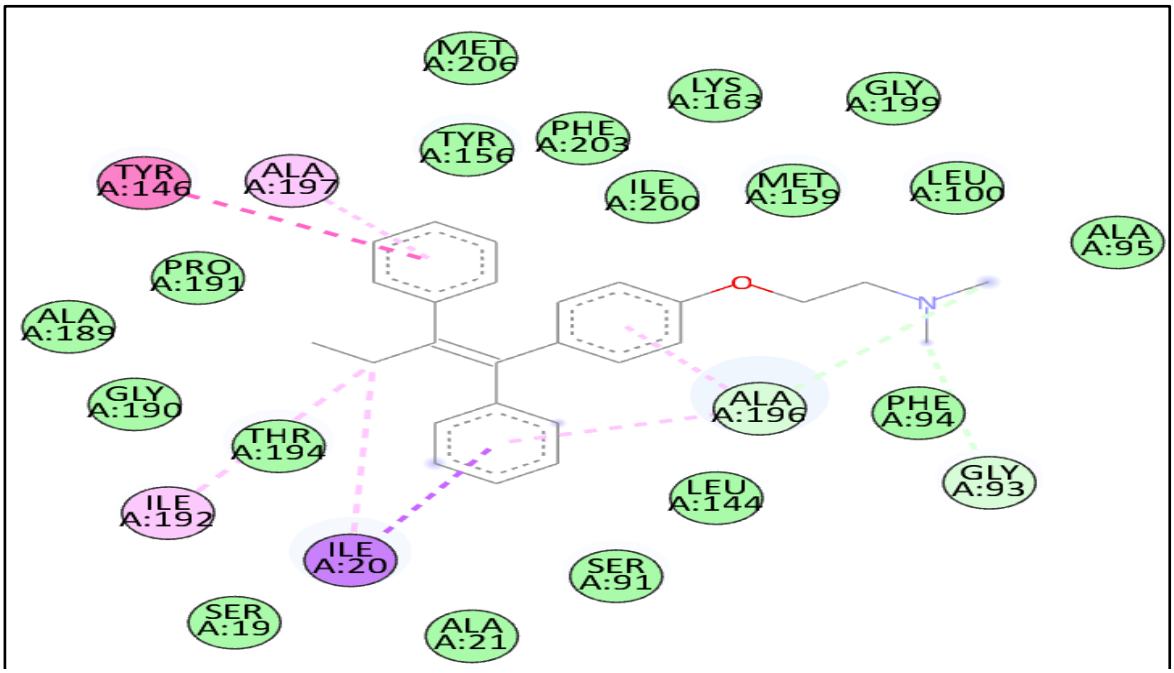

Fig 8:2D Interaction image of 'Tamoxifen' with the Enoyl Reductase

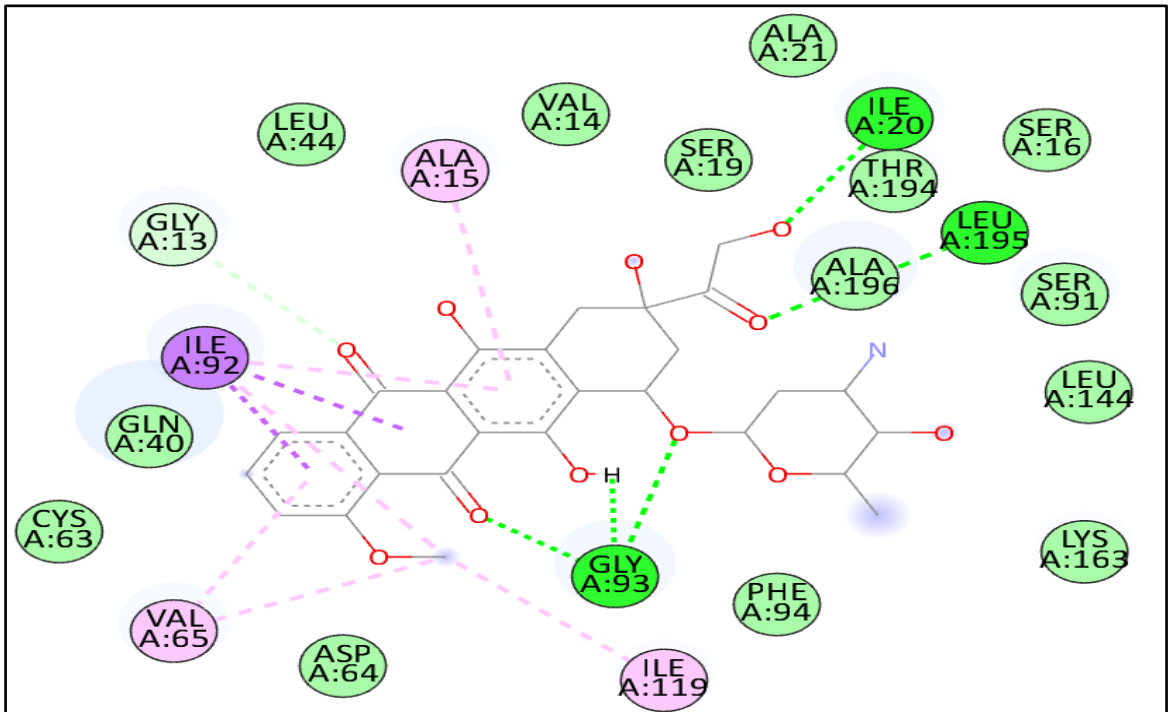

Fig 9:2D Interaction image of 'doxorubicin' with the Enoyl Reductase

Docking studies against RdRp OF HCV (NS5B) protein:

Molecular docking investigations were performed on the novel derivatives (**9a-h**) along with the standard reference drugs Sofosbuvir[35] and Ribavirin[36], against the NS5B protein (PDB ID: 3UPI)[37]. The NS5B protein is the RNA-dependent RNA polymerase (RdRp) of the Hepatitis C Virus (HCV), a critical enzyme in the replication of Hepatitis C Virus (HCV), is vital for the synthesis of the viral RNA genome[38]. Over expression and activity of this enzyme are essential for the viral lifecycle, supporting the rapid replication and persistence of the virus within host cells[39]. Targeting NS5B polymerase with specific inhibitors can effectively disrupt viral replication by limiting RNA synthesis, thereby inhibiting the proliferation of HCV and promoting viral clearance. This makes NS5B polymerase a promising therapeutic target.

All the compounds (**9a-h**) displayed binding energies ranging from -9.4 Kcal/mol to -10.7 kcal/mol, which is superior to the binding energy of the standard reference drugs Sofosbuvir (-8.6 KCal/mol)andRibavirin(-6.3 KCal/mol) were represented in **Table-2**. Notably, compounds 9f, 9c, and 9g scored binding energies of -10.7, -10.6, and -10.6 Kcal/mol respectively, displaying their superior binding affinities. This can be attributed to the conventional hydrogen bonding interactions, carbon-hydrogen bonding, pi-sigma, pi-anion, pi-cation, pi-alkyl, and Vanderwaals interactions between the novel compounds and the RdRp OF HCV (NS5B).

Table-2: Molecular Docking Studies-Hepatitis-c

Molecule	B.E	Interacting A.A Residues	
		H-Bonding	Other types of Interactions
9a	**-10.0**	LEU 159, ASP 318	ARG 48, VAL 52, ARG 158, ILE 160, ASP 220, CYS 223, PHE 224, ASP 225, SER 226, SER 282, THR 287, SER 288, ASN 291, GLY 317, ASP 318, ASP 319, THR 364, SER 367, SER 556
9b	**-10.4**	ARG 158	VAL 52, LYS 141, LEU 159, ILE 160, PHE 193, ASP 220, THR 221, CYS 223, PHE 224, ASP 225, SER 282, THR 287, ASN 291, ASN 316, GLY 317, ASP 318, ASP 319, CYS 366, TYR 448, SER 556, GLY 557
9c	**-9.4**	LYS 141, ARG 386, GLN 446	GLU 143,PHE 193, ARG 200, ASN 316, ASP 319, CYS 366, SER 367, SER 368, ARG 394, ASN 411, MET 414, TYR 415, ILE 447, TYR 448, GLY 449, SER 556,
9d	**-10.2**	ASN 411	PHE 145, LYS 155, ARG 158, PHE 193, PRO 197, ARG 200, CYS 366, SER 367, SER 368, LEU 384, ARG 386, THR 390, PRO 391, ARG 394, GLY 410, MET 414, TYR 415, GLN 446, TYR 448, GLY 449, SER 556
9e	**-10.7**	ASN 316, GLY 449	PHE 193, PRO 197, ARG 200, ASP 225, SER 282, THR 287, SER 288, ASN 291, GLY 317, ASP 319, CYS 366, SER 367, SER 368, LEU 384,GLY 410, ASN 411, MET 414, TYR 415, GLN 446, ILE 447, TYR 448, SER 556
9f	**-10.6**	GLN 446, SER 556, ASP 559	PRO 93, HIS 95, SER 96, LYS 141, GLU 143, ILE 160, PHE 162, ARG 168, GLY 283, PRO 404, ILE 405, ASP 444, CYS 451, GLY 557, ILE 560
9g	**-9.9**	LYS 141, LEU 159, SER 282	ARG 48, VAL 52, ARG 158, ILE 160, PHE 193, SER 218, TYR 219, ASP 220, THR 221, CYS 223, PHE 224, ASP 225, SER 226, THR 287, SER 288, ASN 291,

			GLY 317, ASP 318, ASP 319, LEU 320, SER 556
9h	**-10.5**	ARG 158, SER 367, ARG 394, ASN 411	LYS 141, GLU 143, PHE 145, PHE 193, PRO 197, ARG 200, ASP 319, CYS 366, SER 368, LEU 384, ARG 386, THR 390, GLY 410, MET 414, TYR 415, TYR 448, GLY 449, SER 556
Ribavirin	**--6.3**	TYR 4, LEU 159, ASP 318,	VAL 52, ARG 158, ILE 160, THR 221, CYS 223, PHE 224, ASP 225, SER 226, CYS 279, SER 282,
Sofosbuvir	**-8.6**	ARG 386, TYR 448,	PHE 193, PRO 197, ARG 200, ASN 316, ASP 319, CYS 366, SER 368, LEU 384, THR 390, PRO 391, ARG 394, SER 407, GLY 410, ASN 411, MET 414, TYR 415, GLN 446, ILE 447,

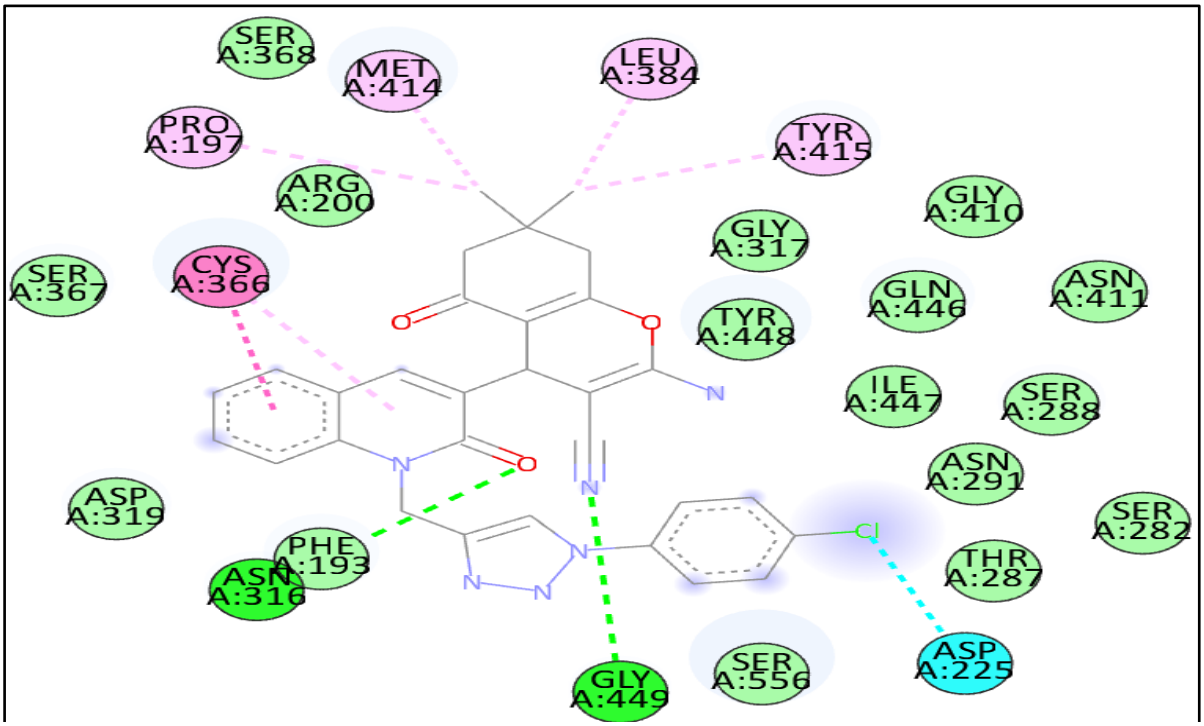

Fig 10:2D Interaction image of '9e' with the RdRp OF HCV (NS5B)

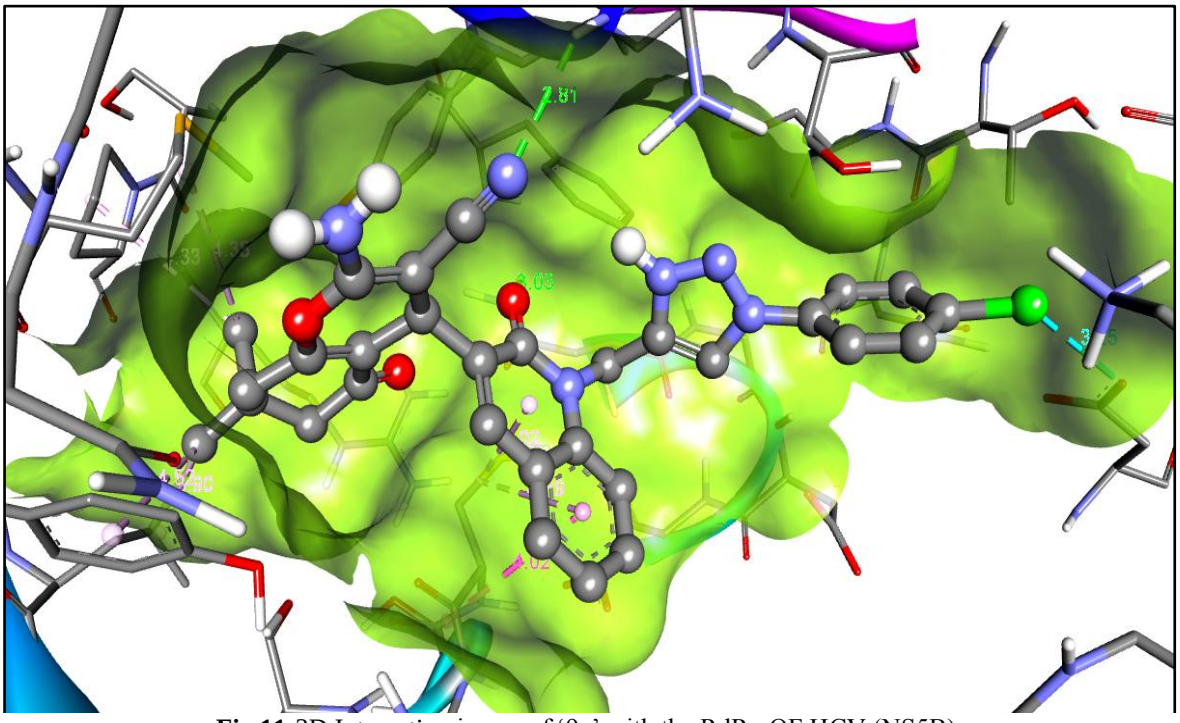

Fig 11:3D Interaction image of '9e' with the RdRp OF HCV (NS5B)

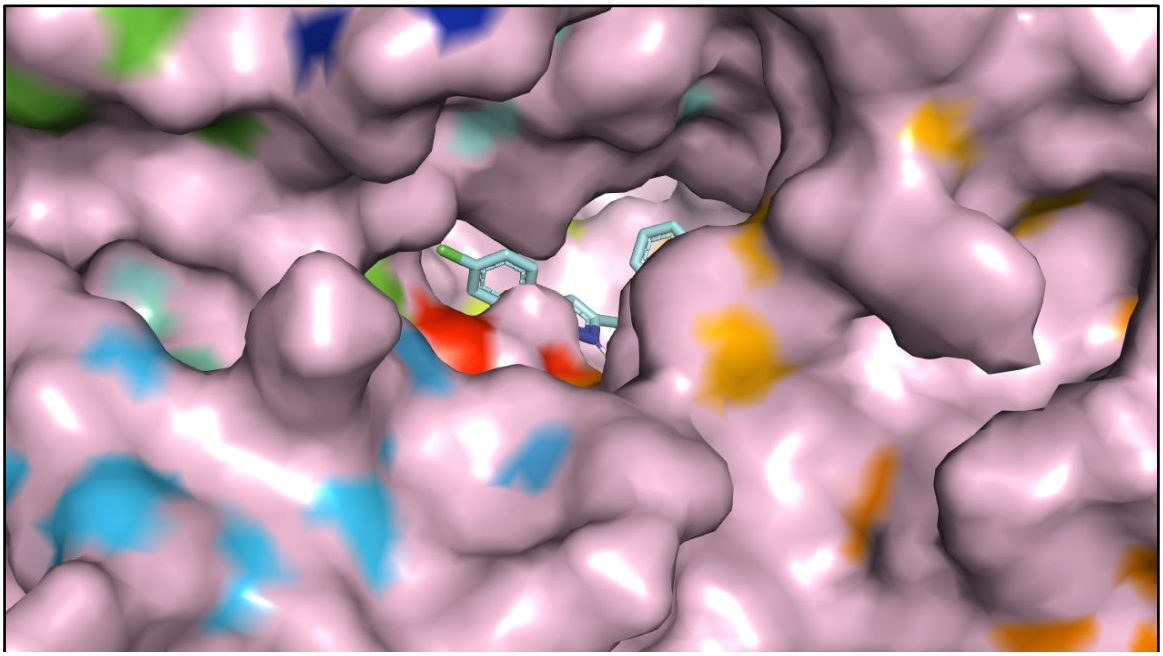

Fig 12:'9e' in the binding pocket of RdRp OF HCV (NS5B)

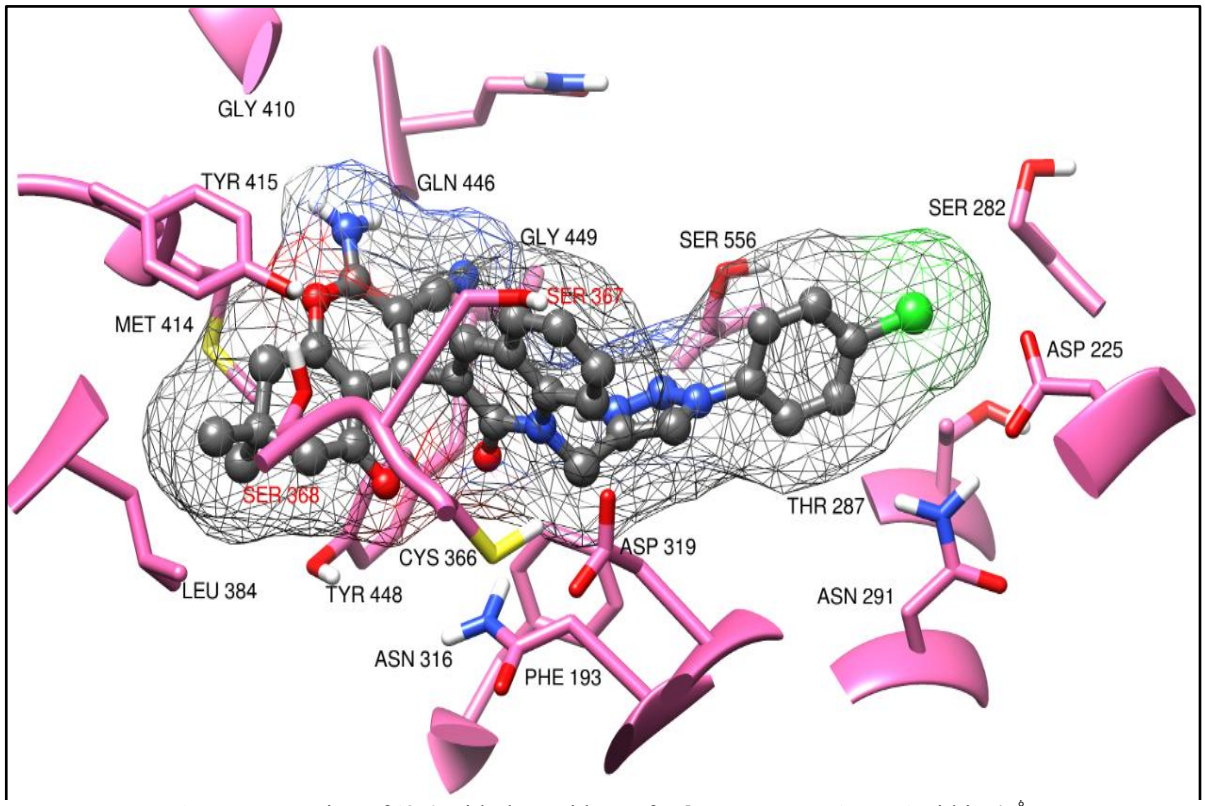

Fig 13: Interaction of '9e' with the residues of RdRp OF HCV (NS5B)within 4 Å

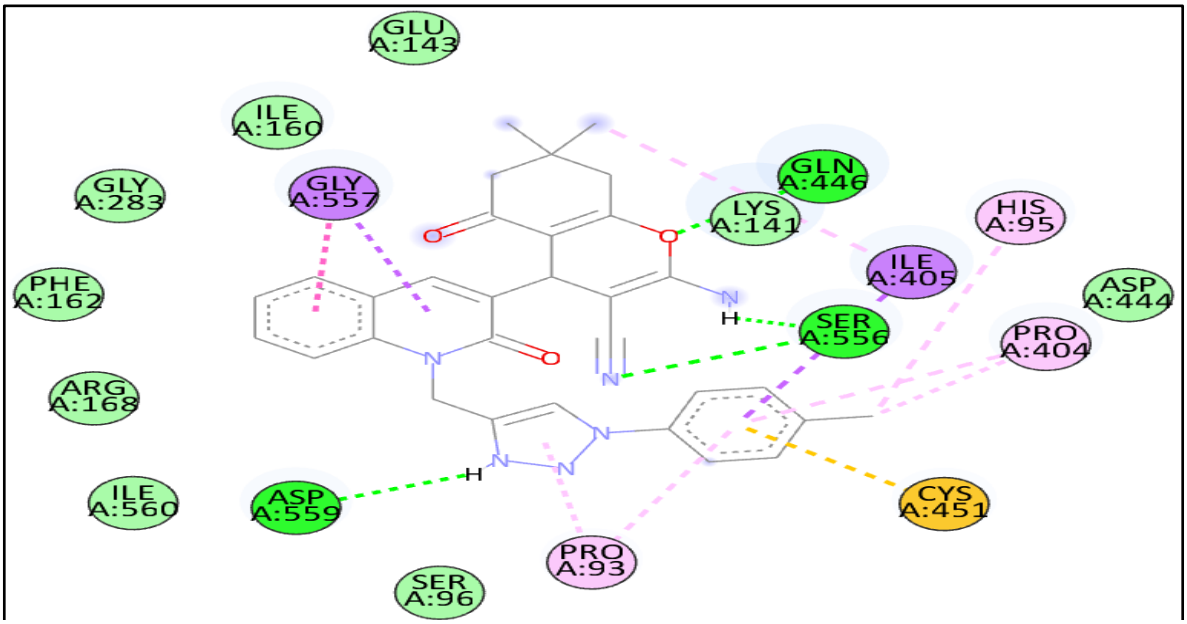

Fig 14:2D Interaction image of '9f' with the RdRp OF HCV (NS5B)

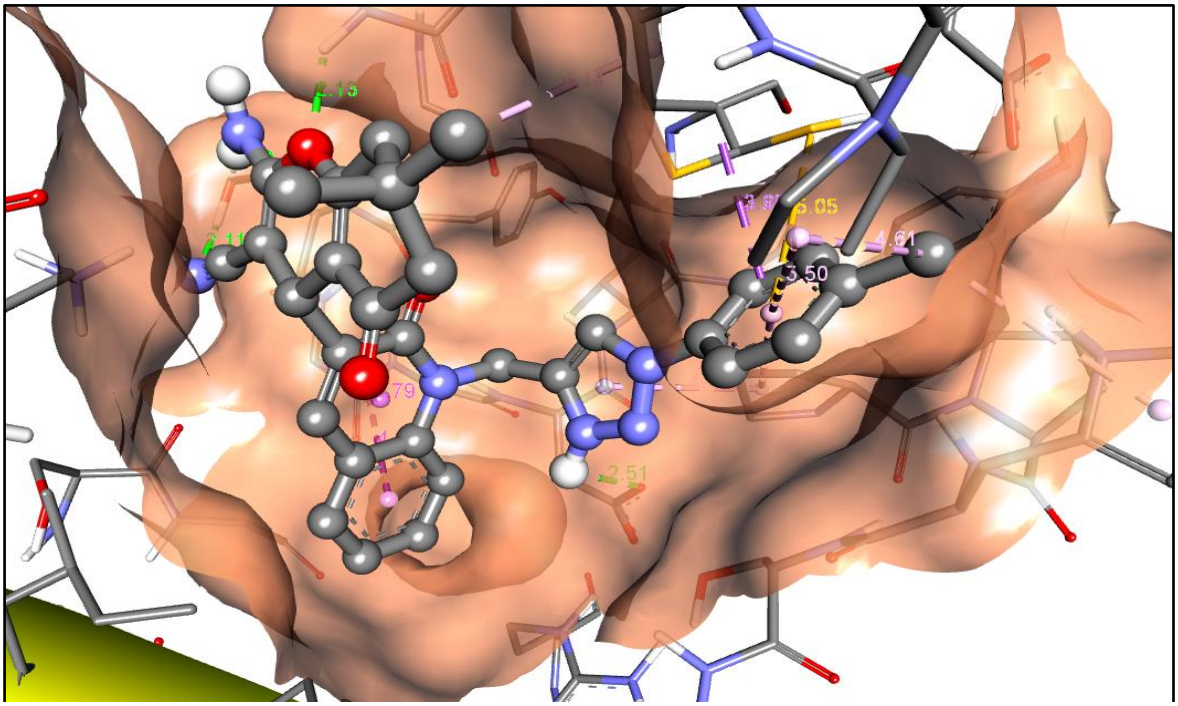

Fig 15:3D Interaction image of 9f' with the RdRp OF HCV (NS5B)

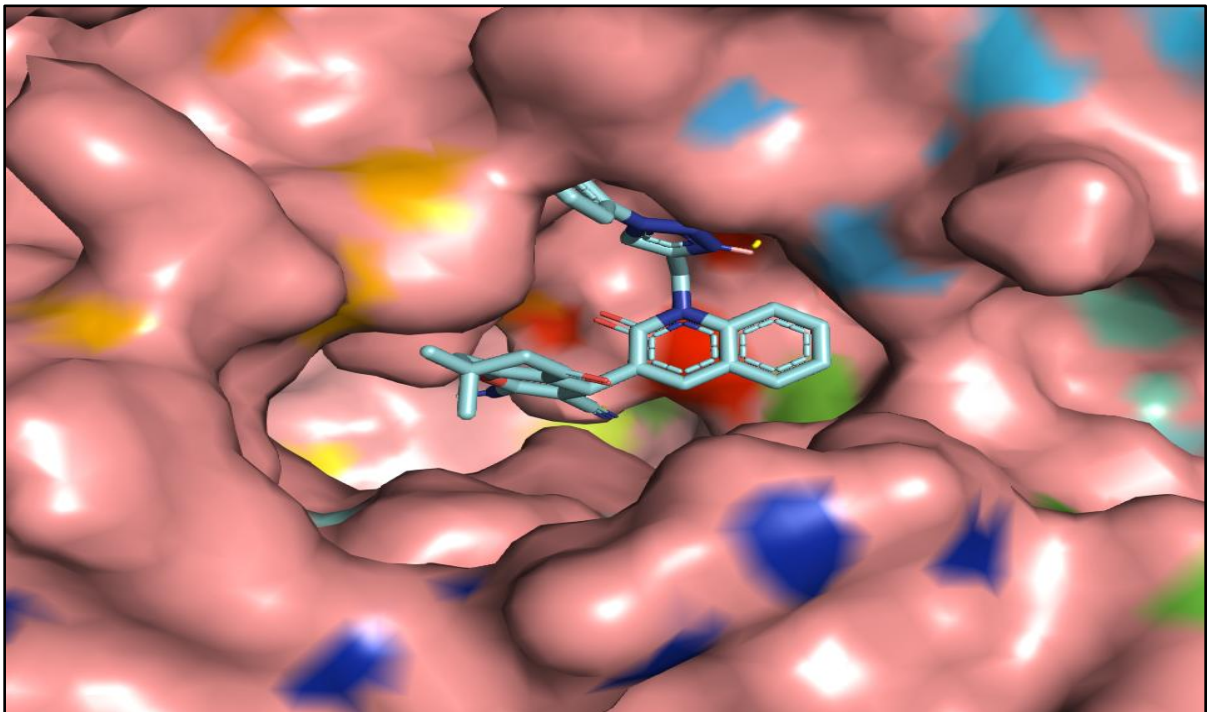

Fig 16:'9f' in the binding pocket of RdRp OF HCV (NS5B)

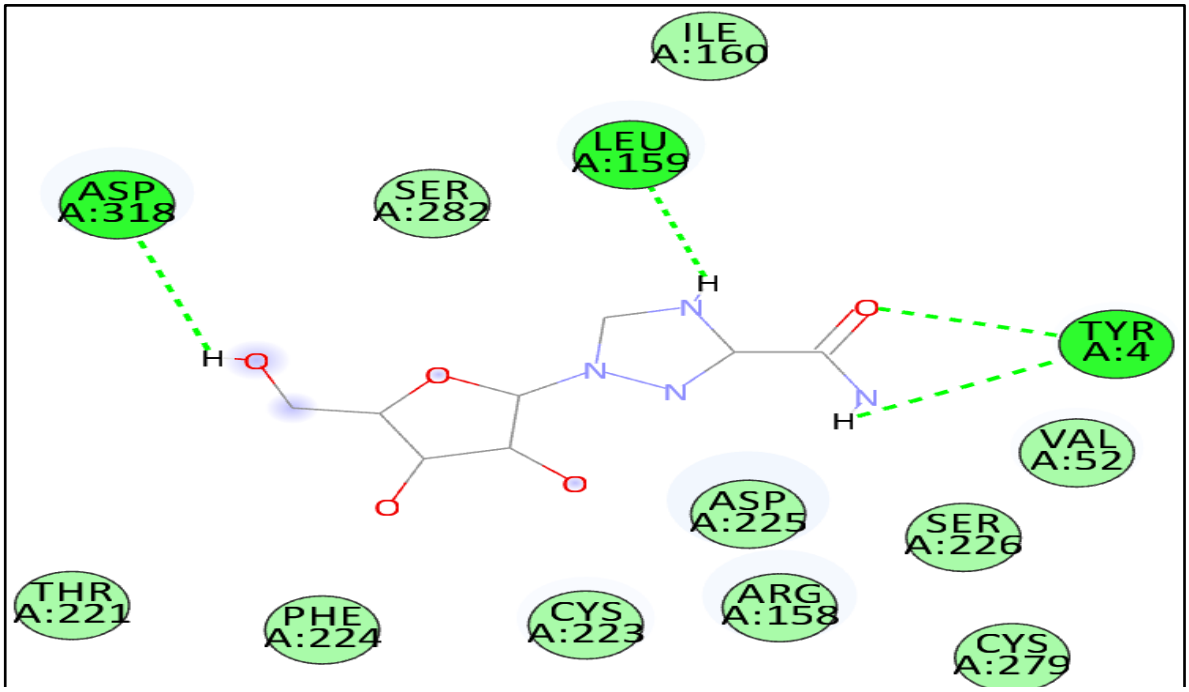

Fig 17:2D Interaction image of '**Ribavirin**' with the RdRp OF HCV (NS5B)

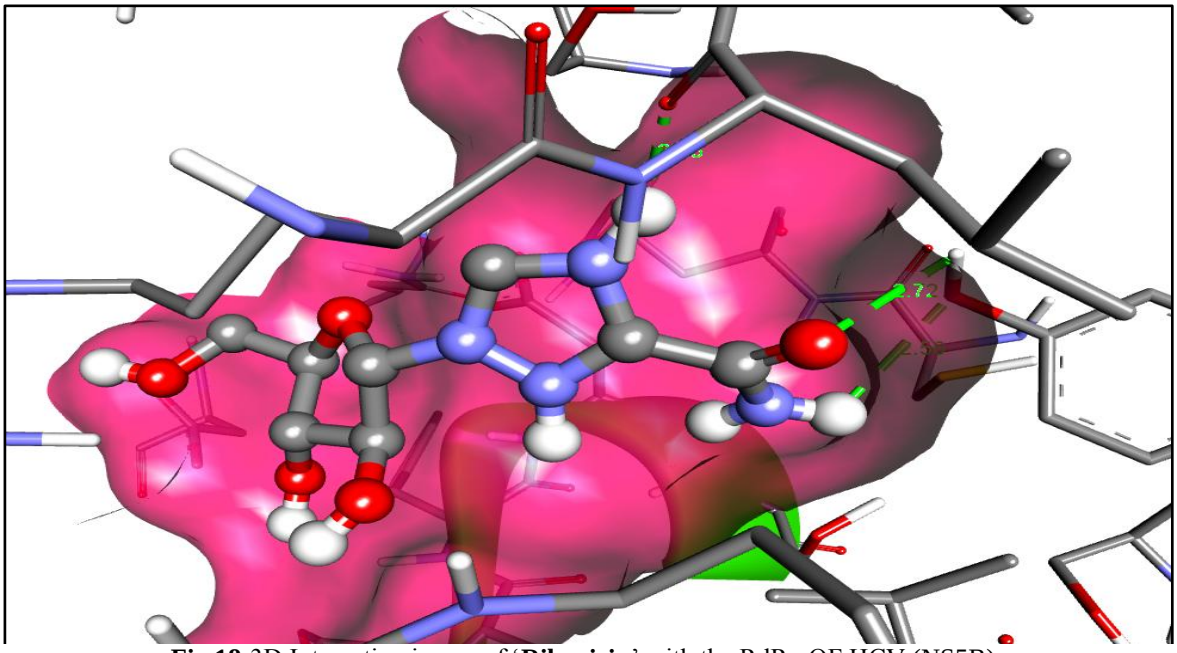

Fig 18:3D Interaction image of '**Ribavirin**' with the RdRp OF HCV (NS5B)

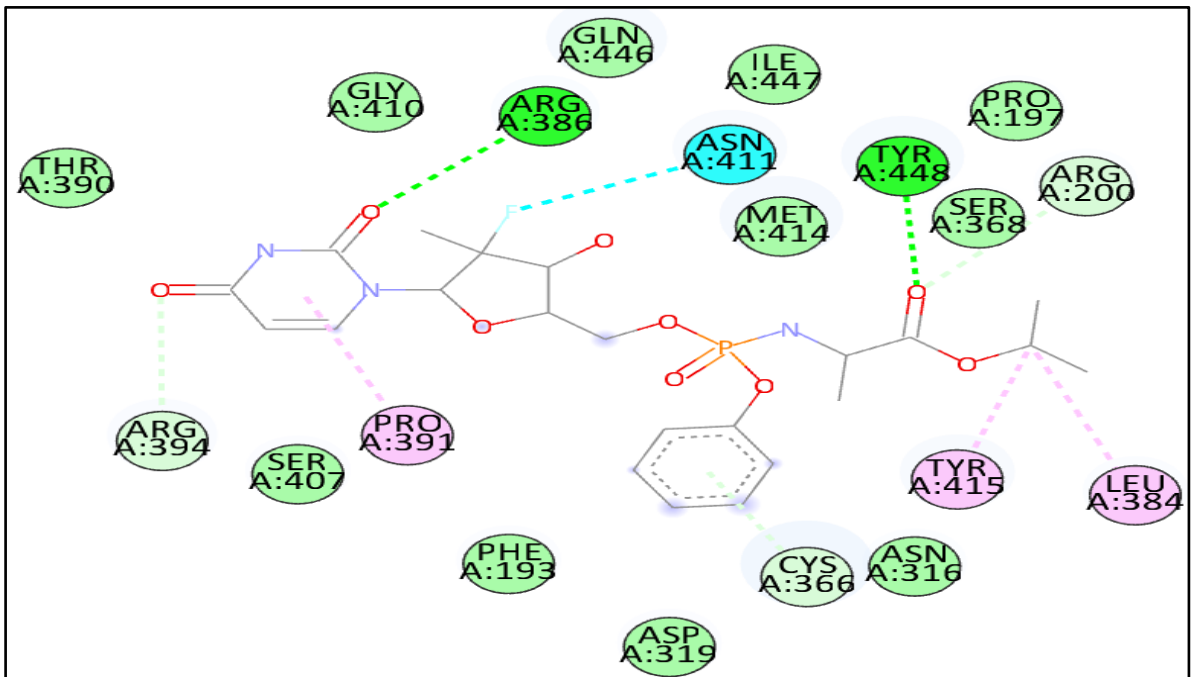

Fig 19:2D Interaction image of '**Sofosbuvir**' with the RdRp OF HCV (NS5B)

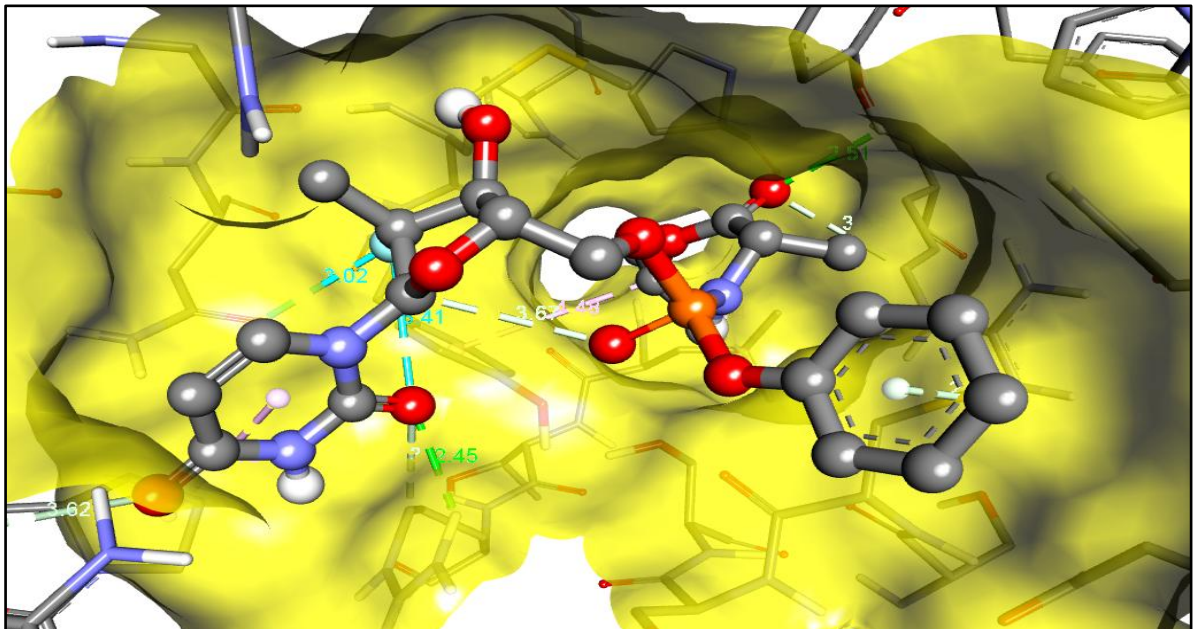

Fig 20:3D Interaction image of '**Sofosbuvir**' with the RdRp OF HCV (NS5B)

III. Conclusion

In this conclusion, we have synthesized novel hybrid molecules **(9a-h**) and examined their anticancer activity against MCF-7 and HepG-2cell lines. Among the hybrid compounds tested, **9d,9f**, **9g,**and **9ef** which contain meta-dichloro**,** para-methyl, meta-dimethoxy and para-chloro substitutions respectively, exhibited significant suppression of MCF-7 and HepG-2 cells, with IC50 values that are notably comparable to those of the standard drug doxorubicin. Conversely, the remaining compounds in the series displayed only mild to moderate activity against the tested cell lines. Additionally, molecular docking studies were conducted on enoyl-ACP reductase and RdRp OF HCV (NS5B).utilizing the AutoDock Vina tool within PyRx. Notably, compounds **9d**, **9f,9g**and **9e** scored binding energies against enol-ACP reductase displaying their superior binding affinities while **9d** showed enhanced affinity against RdRp of HCV.The binding energies and interactions obtained from the docking results corroborated the investigational data. Thus, the synthesized derivatives **9d** and **9f** displayed anticancer properties with excellent binding efficacy.

Experimental Data:

All the chemicals were purchased from different chemical vendors used without further purifications. The solvents used in the reactions and column chromatography were purified and dried. 60–120 mesh (Merk) was used as stationary phase and ethyl acetate and pet ether mixture were used as mobile phase solvents. Instruments like Shimazu 400 MHz were used for ^{1}H NMR and 100 MHz were used for ^{13}C NMR analysis. Mass spectrum of compounds was recorded by using ESI-APCI method. The melting point were recorded on 350 DerajatCelcius di kenarocks123.

Synthesis of2-hydroxyquinoline-3-carbaldehyde(2).

The synthesis of 2-hydroxyquinoline-3-carbaldehyde(2)2-chloroquinoline-3-carbaldehyde (1)(1mmol) was refluxed in 70% acetic acid (5vol) for 6 hrs to obtain 2-hydroxyquinoline-3-carbaldehyde(2).

Synthesis of 2-oxo-1-(prop-2-yn-1-yl)-1,2-dihydroquinoline-3-carbaldehyde(4).

Synthesis of the compound(4) from the 2-hydroxyquinoline-3-carbaldehyde(2)(1mmol) was allowed to react with propargyl bromide(3)(1.2mmol) in DMF using K_2CO_3 at rtfor 4hrs to yielded 2-oxo-1-(prop-2-yn-1-yl)-1,2-dihydroquinoline-3-carbaldehyde(4).

Synthesis of 2-amino-7,7-dimethyl-5-oxo-4-(2-oxo-1-(prop-2-yn-1-yl)-1,2-dihydroquinolin-3-yl)-5,6,7,8-tetrahydro-4H-chromene-3-carbonitrile(7).

Synthesis of the compound (7) from the compound (4)(1mmol) was reacted with 5,5-dimethylcyclohexane-1,3-dione(5)(1mmo), Malononitrile(6)(1.2mmol) inpresence of ethanol and catalytical amount of piperzine rt for 1 hr to yielded of cyclization products of 2-amino-7,7-dimethyl-5-oxo-4-(2-oxo-1-(prop-2-yn-1-yl)-1,2-dihydroquinolin-3-yl)-5,6,7,8-tetrahydro-4H-chromene-3-carbonitrile(7).

General procedure for synthesis of 2-amino-7,7-dimethyl-5-oxo-4-(2-oxo-1-((subtituted-phenyl-1H-1,2,3-triazol-4-yl)methyl)-1,2-dihydroquinolin-3-yl)-5,6,7,8-tetrahydro-4H-chromene-3-carbonitrile(9a-h)

The synthesis title compounds 2-amino-7,7-dimethyl-5-oxo-4-(2-oxo-1-((subtituted-phenyl-1H-1,2,3-triazol-4-yl)methyl)-1,2-dihydroquinolin-3-yl)-5,6,7,8-tetrahydro-4H-chromene-3-carbonitrile(9a-i) from

theterminalalkyne compound (7)(1mmol) on further reaction with various substituted aryl azides(**8a-h**)(1.2mmol) in click reactionresulted respective2-amino-7,7-dimethyl-5-oxo-4-(2-oxo-1-((subtituted-phenyl-1H-1,2,3-triazol-4-yl)methyl)-1,2-dihydroquinolin-3-yl)-5,6,7,8-tetrahydro-4H-chromene-3-carbonitrile(**9a-h**), the products were obtained in good yields.

Spectral data:

2-amino-4-(1-((1-(4-bromophenyl)-1H-1,2,3-triazol-4-yl)methyl)-2-oxo-1,2-dihydroquinolin-3-yl)-7,7-dimethyl-5-oxo-5,6,7,8-tetrahydro-4H-chromene-3-carbonitrile(9a)

^{1}H NMR (400 MHz, $CDCl_3$) δ 7.77 (s, 1H), 7.57 (d, *J* = 11.7 Hz, 5H), 7.46 (d, *J* = 8.8 Hz, 2H), 7.24 – 7.20 (m, 1H), 6.91 (d, *J* = 8.8 Hz, 2H), 4.62 (d, *J* = 13.0 Hz, 2H), 2.49 (s, 2H), 2.32 – 2.17 (m, 2H), 1.12 (s, 3H), 1.05 (s, 3H).^{13}C NMR (101 MHz, $CDCl_3$) δ 196.32, 163.55, 160.94, 159.12, 139.24, 138.67, 138.26, 135.90, 132.80, 131.45, 130.72, 129.14, 122.63, 122.33, 121.48, 120.70, 117.76, 114.68, 111.33, 50.72, 40.64, 38.42, 33.70, 32.18, 29.31, 27.12.

2-amino-4-(1-((1-(4-iodophenyl)-1H-1,2,3-triazol-4-yl)methyl)-2-oxo-1,2-dihydroquinolin-3-yl)-7,7-dimethyl-5-oxo-5,6,7,8-tetrahydro-4H-chromene-3-carbonitrile(9b)

^{1}H NMR (400 MHz, $CDCl_3$) δ 8.09 (d, *J* = 1.8 Hz, 1H), 7.85 – 7.72 (m, 3H), 7.67 – 7.60 (m, 1H), 7.56 (t, *J* = 8.1 Hz, 1H), 7.47 – 7.41 (m, 1H), 7.22 (d, *J* = 7.7 Hz, 1H), 6.83 (dd, *J* = 36.0, 8.5 Hz, 1H), 5.33 – 4.86 (m, 2H), 4.70 (s, 2H), 4.41 (s, 1H), 2.45 (dd, *J* = 38.6, 17.8 Hz, 2H), 2.20 (dt, *J* = 16.1, 8.2 Hz, 2H), 1.09 (s, 3H), 1.01 (s, 3H).^{13}C NMR (101 MHz, $CDCl_3$) δ 196.32, 163.54, 160.94, 159.06, 138.67, 138.26, 135.44, 134.44, 131.43, 130.72, 129.83, 129.14, 122.62, 121.58, 120.57, 114.67, 111.36, 50.72, 40.66, 38.42, 33.67, 32.19, 29.31, 27.11.

2-amino-7,7-dimethyl-4-(1-((1-(4-nitrophenyl)-1H-1,2,3-triazol-4-yl)methyl)-2-oxo-1,2-dihydroquinolin-3-yl)-5-oxo-5,6,7,8-tetrahydro-4H-chromene-3-carbonitrile(9c)

^{1}H NMR (300 MHz, $CDCl_3$) δ 8.34 (d, *J* = 8.8 Hz, 2H), 8.19 (s, 1H), 7.93 (d, *J* = 8.8 Hz, 2H), 7.76 (d, *J* = 8.2 Hz, 1H), 7.68 (s, 1H), 7.54 (t, *J* = 8.1 Hz, 2H), 7.22 (t, *J* = 7.5 Hz, 1H), 5.69 (d, *J* = 29.6 Hz, 2H), 5.30 (s, 1H), 4.72 (d, *J* = 17.5 Hz, 2H), 2.48 (s, 2H), 2.22 (t, *J* = 14.0 Hz, 2H), 1.12 (s, 3H), 1.06 (s, 3H).^{13}C NMR (101 MHz, $CDCl_3$) δ 196.29, 163.53, 161.04, 158.86, 147.12, 141.09, 138.49, 137.95, 130.79, 129.14, 125.44, 122.73, 120.62, 120.42, 114.52, 111.51, 50.73, 40.69, 38.34, 32.24, 29.23, 27.32.

2-amino-4-(1-((1-(3,5-dichlorophenyl)-1H-1,2,3-triazol-4-yl)methyl)-2-oxo-1,2-dihydroquinolin-3-yl)-7,7-dimethyl-5-oxo-5,6,7,8-tetrahydro-4H-chromene-3-carbonitrile(9d)

^{1}H NMR (300 MHz, $CDCl_3$) δ 8.11 – 8.04 (m, 1H), 7.91 (d, *J* = 8.4 Hz, 1H), 7.65 (dd, *J* = 18.7, 6.8 Hz, 2H), 7.58 – 7.46 (m, 2H), 7.20 (d, *J* = 10.3 Hz, 1H), 7.00 (s, 1H), 5.30 (s, 2H), 5.13 (s, 1H), 4.45 (q, *J* = 7.0 Hz, 2H), 2.60 (d, *J* = 3.8 Hz, 2H), 2.48 – 2.41 (m, 2H), 1.42 (t, *J* = 7.1 Hz, 3H), 1.20 – 1.03 (m, 3H).^{13}C NMR (101 MHz, $CDCl_3$) δ 196.36, 163.57, 160.85, 159.13, 138.81, 138.51, 134.72, 130.70, 130.15, 129.17, 122.56, 120.38, 114.77, 113.09, 111.26, 50.72, 40.67, 34.18, 32.20, 29.43, 26.97, 21.10.

2-amino-4-(1-((1-(4-chlorophenyl)-1H-1,2,3-triazol-4-yl)methyl)-2-oxo-1,2-dihydroquinolin-3-yl)-7,7-dimethyl-5-oxo-5,6,7,8-tetrahydro-4H-chromene-3-carbonitrile(9e)

^{1}H NMR (300 MHz, $CDCl_3$) δ 7.78 (d, *J* = 17.7 Hz, 2H), 7.54 (d, *J* = 8.2 Hz, 4H), 7.26 (s, 2H), 6.95 (d,*J* =8.2 Hz, 1H),5.30 (s,1H), 4.85–4.37 (m, 3H), 3.83(s, 2H), 2.44 (s, 2H), 2.21 (d,*J* = 5.1Hz,2H),1.05(d, *J*=23.0Hz,6H).^{13}C NMR (101 MHz, $CDCl_3$) δ 196.95, 169.41, 140.50, 137.76, 137.14, 133.99, 131.81, 128.48, 127.30, 126.31, 125.89, 124.64, 124.33, 121.24, 111.22, 91.22, 52.05, 43.05, 31.53, 29.39, 26.90, 21.73.

2-amino-7,7-dimethyl-5-oxo-4-(2-oxo-1-((1-(p-tolyl)-1H-1,2,3-triazol-4-yl)methyl)-1,2-dihydroquinolin-3-yl)-5,6,7,8-tetrahydro-4H-chromene-3-carbonitrile(9f)

^{1}H NMR (300 MHz, $CDCl_3$) δ 7.91 – 7.79 (m, 2H), 7.76 (s, 1H), 7.58 (d, *J* = 8.1 Hz, 2H), 7.51 (d, *J* = 8.4 Hz, 3H), 7.24 – 7.16 (m, 2H), 5.64 (d, *J* = 29.5 Hz, 2H), 5.30 (s, 2H), 4.61 (d, *J* = 40.7 Hz, 2H), 2.47 (s, 2H), 2.38 (s, 3H), 2.22 (q, *J* = 16.4 Hz, 2H), 1.10 (s, 3H), 1.02 (s, 3H).^{13}C NMR (101 MHz, $CDCl_3$) δ 196.36, 163.57, 160.85, 159.13, 138.81, 138.51, 134.72, 130.89, 130.70, 130.15, 129.17, 122.56, 120.54, 120.38, 114.77, 111.26, 50.72, 40.67, 34.18, 32.20, 29.43, 26.97, 21.10.

2-amino-4-(1-((1-(4-methoxyphenyl)-1H-1,2,3-triazol-4-yl)methyl)-2-oxo-1,2-dihydroquinolin-3-yl)-7,7-dimethyl-5-oxo-5,6,7,8-tetrahydro-4H-chromene-3-carbonitrile(9g)

^{1}H NMR (300 MHz, $CDCl_3$) δ 7.78 (d, *J* = 17.7 Hz, 2H), 7.68 – 7.50 (m, 4H), 7.45 (d, *J* = 8.5 Hz, 1H), 7.20 (d, *J* = 7.1 Hz, 1H), 6.95 (d, *J* = 8.2 Hz, 1H), 5.30 (s, 2H), 5.02 (dd, *J* = 57.4, 17.3 Hz, 1H), 4.81 – 4.39 (m, 3H), 3.83 (s, 2H), 2.58 – 2.35 (m, 2H), 2.36 – 2.09 (m, 2H), 1.09 (s, 3H), 1.01 (s, 3H).^{13}C NMR (101 MHz, $CDCl_3$) δ 196.74, 163.87, 163.58, 159.86, 159.53, 147.48, 147.35, 138.82, 138.74, 138.45, 138.35, 130.41, 129.45, 129.15, 122.57, 121.94, 120.56, 114.65, 114.22, 110.76, 50.76, 40.65, 35.22, 32.26, 31.65, 29.23, 27.16.

2-amino-4-(1-((1-(4-bromo-2-fluorophenyl)-1H-1,2,3-triazol-4-yl)methyl)-2-oxo-1,2-dihydroquinolin-3-yl)-7,7-dimethyl-5-oxo-5,6,7,8-tetrahydro-4H-chromene-3-carbonitrile(9h)

^{1}H NMR (400 MHz, $CDCl_3$) δ 7.99 (s, 1H), 7.87 – 7.73 (m, 2H), 7.57 (dd, *J* = 15.4, 6.8 Hz, 2H), 7.43 (d, *J* = 7.7 Hz, 2H), 7.21 (d, *J* = 7.3 Hz, 1H), 6.94 (t, *J* = 8.7 Hz, 1H), 5.30 (s, 2H), 4.73 (s, 2H), 4.45 (d, *J* = 29.0 Hz, 1H), 2.44 (d, *J* = 15.1 Hz, 2H), 2.20 (dd, *J* = 38.0, 16.6 Hz, 2H), 1.10 (s, 3H), 1.00 (s, 3H).^{13}C NMR (101 MHz,

$CDCl_3$) δ 196.50, 164.14, 163.66, 160.77, 159.32, 138.86, 138.72, 130.68, 129.28, 128.66, 125.74, 124.45, 124.42, 122.71, 122.60, 120.71, 120.48, 114.65, 114.23, 50.71, 40.65, 34.59, 32.17, 29.41, 27.15, 26.84.

Anti-cancer activity using MTT assay:

The cancer cells were appropriately plated and cultured (100 µL per well) in clear bottom 96-well tissue culture plates with a concentration of 10^5 cells per well. The test samples were added to the well plates with triplicate concentrations ranging from 5 to 100 µM (5, 10, 20, 40, 60, 80, and 100µM). After 24 hr seeding, the cells were incubated for 72 h. The cells were incubated for another 72 h. The cells in the well were washed twice with phosphate buffer solution, and 20 µL of the MTT staining solution (5 mg/mL in phosphate buffer solution) was added to each well, and the plate was incubated at 37 °C. After 4 h, 100 µL of dimethyl sulfoxide (DMSO) was added to each well to dissolve the formazan crystals, and absorbance was recorded with a 570 nm using a microplate reader. The IC_{50} values were calculated using graph Pad Prism Version 5.1.

Docking Experimental:

The protein structure was obtained from RCSB PDB Database[40]. Water molecules and other entities were cleaned from the protein using Discovery Studio Visualize[41].ChemDraw software was used to draw the molecular structures of compounds 9a-i, the standard drug Doxorubicin. The Docking operations were performed using PyRx, a virtual screening software[42].Visualization of the interactions of the ligands with the target protein was done using Pymol[43] and Discovery Studio Visualizer. The results are tabulated.

Acknowledgements

All the authors are thankful to the Head, Department of chemistry, Osmania University, Hyderabad for providing laboratory facilities. We thank Central Facilities and Research Development (CFRD) analytical team for providing spectral analytical facilities.

Conflict of interest

All authors declare that there is no conflict of interest.

References

[1]. U. Shah, A. Patel, S. Patel, M. Patel, A. Patel, S.P. Patel, S. Patel, R. Maheshwari, A. G Mtewa, K. Gandhi. Role of Natural and Synthetic Flavonoids as Potential Aromatase Inhibitors in Breast Cancer: Structure-Activity Relationship Perspective. Anti-Cancer Agents in Medicinal Chemistry. 2022: 22 (11); 2063-2079.

[2]. Arnold M; Morgan E; Rumgay H; Mafra A; Singh D; Laversanne M; Vignat J; Gralow JR; Cardoso F; Siesling S; Soerjomataram I. Current and future burden of breast cancer: Global statistics for 2020 and 2040. Breast. 2022; 66:15-23.

[3]. Keuper K, Bartek J, Maya-Mendoza A. The nexus of nuclear envelope dynamics, circular economy and cancer cell pathophysiology. Eur J Cell Biol. 2024 Jun;103(2):151394.

[4]. Guardiola S, Varese M, Sánchez-Navarro M, Giralt E. A Third Shot at EGFR: New Opportunities in Cancer Therapy. Trends Pharmacol Sci. 2019 Dec;40(12):941-955.

[5]. Ashwag S. Alanazi, Tebyan O. Mirgany, Nawaf A. Alsaif, Aisha A. Alsfouk, Mohammed M. Alanazi. Design, synthesis, antitumor evaluation, and molecular docking of novel pyrrolo[2,3-d]pyrimidine as multi-kinase inhibitors. Saudi Pharmaceutical Journal, 2023; 31(6): 989-997.

[6]. Robert Roskoski. Small molecule inhibitors targeting the EGFR/ErbB family of protein-tyrosine kinases in human cancers. Pharmacological Research,2019; 139: 395-411.

[7]. Lorscheider, M.; Gaudin, A.; Nakhlé, J.; Veiman, K.-L.; Richard, J.; Chassaing, C. Challenges and Opportunities in the Delivery of Cancer Therapeutics: Update on Recent Progress. Therapeutic Delivery. 2021, 12, 55–76.

[8]. Lauria, A.; La Monica, G.; Bono, A.; Martorana, A. Quinoline Anticancer Agents Active on DNA and DNA.Interacting Proteins: From Classical to Emerging Therapeutic Targets. European Journal of Medicinal Chemistry, 2021, 220.

[9]. Qiu C, Tarrant MK, Choi SH, Sathyamurthy A, Bose R, Banjade S, Pal A, Bornmann WG, Lemmon MA, Cole PA, Leahy DJ. Mechanism of activation and inhibition of the HER4/ErbB4 kinase. Structure. 2008 Mar;16(3):460-7.

[10]. Matada GSP, Abbas N, Dhiwar PS, Basu R, Devasahayam G. Design, Synthesis, *In Silico* and *In Vitro* Evaluation of Novel Pyrimidine Derivatives as EGFR Inhibitors. Anticancer Agents Med Chem. 2021;21(4):451-461.

[11]. Lo HW, Hsu SC, Hung MC. EGFR signaling pathway in breast cancers: from traditional signal transduction to direct nuclear translocalization. Breast Cancer Res Treat. 2006 Feb;95(3):211-8.

[12]. Zandi R, Larsen AB, Andersen P, Stockhausen MT, Poulsen HS. Mechanisms for oncogenic activation of the epidermal growth factor receptor. Cell Signal. 2007 Oct;19(10):2013-23.

[13]. Katerina, I.S.; Lozan, T.T.; Nataliya, P.B.; Mauricio, A.P.; Irena, P.K. Developments in the Application of 1,2,3-Triazoles in Cancer Treatment. Recent Patents on Anti-Cancer Drug Discovery 2020, 15, 92–112.

[14]. N.J.P. Subhashini, E.P. Kumar, N. Gurrapu, V. Yerragunta, Design and synthesis of imidazolo-1, 2, 3-triazoles hybrid compounds by microwave-assisted method: evaluation as an antioxidant and antimicrobial agents and molecular docking studies, J. Mol. Struct. 1180 (2019) 618–628.https://doi.org/10.1016/j.molstruc.2018.11.029.

[15]. Brandão, G.C.; Rocha Missias, F.C.; Arantes, L.M.; Soares, L.F.; Roy, K.K.; Doerksen, R.J.; Braga de Oliveira, A.; Pereira, G.R. Antimalarial Naphthoquinones. Synthesis via Click Chemistry, in Vitro Activity, Docking to PfDHODH and SAR of Lapachol-Based Compounds. Eur J Med Chem 2018, 145, 191–205.

[16]. Kaushik, C.P.; Kumar, K.; Lal, K.; Narasimhan, B.; Kumar, A. Synthesis and Antimicrobial Evaluation of 1,4-Disubstituted 1,2,3-Triazoles Containing Benzofused N-Heteroaromatic Moieties. Monatsh Chem 2016, 147, 817–828.

[17]. Nejadshafiee, V.; Naeimi, H.; Zahraei, Z. Efficient Synthesis and Antibacterial Evaluation of Some Substituted β-Hydroxy-1,2,3-Triazoles. Chemical Data Collections 2020, 28.

[18]. Nandikolla, A.; Srinivasarao, S.; Khetmalis, Y.M.; Kumar, B.K.; Murugesan, S.; Shetye, G.; Ma, R.; Franzblau, S.G.; Sekhar, K.V.G.C. Design, Synthesis and Biological Evaluation of Novel 1,2,3-Triazole Analogues of Imidazo-[1,2-a]-Pyridine-3-Carboxamide against Mycobacterium Tuberculosis.Toxicology in Vitro 2021, 74.

[19]. Scarim, C.B.; Pavan, F.R. Thiazole, Triazole, Thio- and Semicarbazone Derivatives - Promising Moieties for Drug Development for the Treatment of Tuberculosis. European Journal of Medicinal Chemistry Reports 2021, 1.

[20]. Praveenkumar E, Nirmala Gurrapu, Prashanth Kumar Kolluri, VishwanadhamYerragunta, Bharathi Reddy Kunduru , Subhashini N.J.P.Synthesis, anti-diabetic evaluation and moleculardocking studies of 4-(1- aryl-1H-1, 2, 3-triazol-4-yl)-1,4- dihydropyridine derivatives as novel 11-β hydroxysteroid dehydrogenase-1 (11β-HSD1) inhibitors.*Bioorganic Chemistry,* 2019, 90, 103056.https://doi.org/10.1016/j.bioorg.2019.103056.

[21]. E. Praveenkumar, Nirmala Gurrapu, Prashanth Kumar Kolluri, Shivaraj, N.J.P.Subhashini, Appaji Dokala.Selective CDK4/6 inhibition of novel 1,2,3-triazole tethered acridinedione derivatives induces G1/S cell cycle transition arrest via Rb phosphorylationlockade in breast cancer models, *Bioorganic Chemistry,* 2021,116, 105377.doi: 0.1016/j.bioorg.2021.105377.

[22]. N. Gurrapu, E.P. Kumar, P.K. Kolluri, S. Putta, S.K. Sivan, N.J.P. Subhashini, Synthesis,biological evaluation and molecular docking studies of novel 1, 2, 3- triazole tethered chalcone hybrids as potential anticancer agents, J. Mol. Struct.2020, 1217, 128356. https://doi.org/10.1016/j.molstruc.2020.128356.

[23]. Dixit, D.; Verma, P.K.; Marwaha, R.K. A Review on 'Triazoles': Their Chemistry, Synthesis and Pharmacological Potentials. J Iran Chem Soc 2021, 18, 2535–2565.

[24]. Bourakadi, K.E.; Mekhzoum, M.E.M.; Saby, C.; Morjani, H.; Chakchak, H.; Merghoub, N.; Qaiss, A.; Kacem, E.; Bouhfid, R. Synthesis, Characterization and in Vitro Anticancer Activity of Thiabendazole Derived 1,2,3-Triazole Derivatives. New J. Chem. 2020, 44, 12099–12106,

[25]. Xu, Z.; Zhao, S.-J.; Liu, Y. 1,2,3-Triazole-Containing Hybrids as Potential Anticancer Agents: Current Developments, Action Mechanisms and Structure-Activity Relationships. Eur J Med Chem 2019, 183.

[26]. Kemnitzer W, Kasibhatla S, Jiang S, Zhang H, Zhao J, Jia S, et al. Discovery of 4-aryl-4H-chromenes as a new series of apoptosis inducers using a cell- and caspase based high-throughput screening assay. 2. Structure activity relationships of the 7- and 5-, 6-, 8-positions. Bioorg Med Chem Lett. 2005;15:4745-51.

[27]. Kemnitzer W, Drewe J, Jiang S, Zhang H, Zhao J, Crogan-Grundy C, et al. Discovery of 4-aryl-4H chromenes as a new series of apoptosis inducers using a cell- and caspase-based high-throughput screening assay. 3. Structure-activity relationships of fused rings at the 7,8-positions. J Med Chem. 2007;50:2858-64.

[28]. Raj Vinit , Lee Jintae, 2H/4H-Chromenes—A Versatile Biologically Attractive Scaffold, Frontiers in Chemistry.8, 2020.

[29]. Patil, S. A., Patil, R., Pfeffer, L. M., & Miller, D. D. (2013). Chromenes: Potential New Chemotherapeutic Agents for Cancer. *Future Medicinal Chemistry*, *5*(14), 1647–1660.

[30]. Patil SA, Wang J, Li XS, Chen J, Jones TS, Hosni-Ahmed A, Patil R, Seibel WL, Li W, Miller DD. New substituted 4H-chromenes as anticancer agents. Bioorg Med Chem Lett. 2012 Jul 1;22(13):4458-61.

[31]. Shou, Jiang, et al. "Mechanisms of tamoxifen resistance: increased estrogen receptor-HER2/neu cross-talk in ER/HER2–positive breast cancer." *Journal of the National Cancer Institute* 96.12 (2004): 926-935.

[32]. Michael J Stewart, Sapan Parikh, Guoping Xiao, Peter J Tonge, Caroline Kisker, Structural basis and mechanism of enoyl reductase inhibition by triclosan11Edited by P. E. Wright, Journal of Molecular Biology, Volume 290, Issue 4,1999, Pages 859-865.

[33]. Heath, Richard J., and Charles O. Rock. "Enoyl-acyl carrier protein reductase (fabI) plays a determinant role in cycles of fatty acid elongation in Escherichia coli (∗)." *Journal of Biological Chemistry* 270.44 (1995): 26538-26542.

[34]. Massengo-Tiassé, R. Prisca, and John E. Cronan. "Diversity in enoyl-acyl carrier protein reductases." *Cellular and molecular life sciences* 66 (2009): 1507-1517.

[35]. Agwupuye, John A., et al. "Molecular modeling and DFT studies of diazenylphenyl derivatives as a potential HBV and HCV antiviral agents." *Chemical Physics Impact* 5 (2022): 100122.

[36]. Muthu, S., et al. "Spectroscopic (FT-IR, FT-Raman) investigation, topology (ESP, ELF, LOL) analyses, charge transfer excitation and molecular docking (dengue, HCV) studies on ribavirin." *Chemical Data Collections* 17 (2018): 236-250.

[37]. PDB DOI: https://doi.org/10.2210/pdb3UPI/pdb.

[38]. Lohmann, Volker, et al. "Biochemical properties of hepatitis C virus NS5B RNA-dependent RNA polymerase and identification of amino acid sequence motifs essential for enzymatic activity." *Journal of virology* 71.11 (1997): 8416-8428.

[39]. Luo, Guangxiang, et al. "De novo initiation of RNA synthesis by the RNA-dependent RNA polymerase (NS5B) of hepatitis C virus." *Journal of virology* 74.2 (2000): 851-863.

[40]. Rose, Y., Duarte, J.M., Lowe, R., Segura, J., Bi, C., Bhikadiya, C., Chen, L., Rose, A.S., Bittrich, S., Burley, S.K. and Westbrook, J.D., 2021. RCSB Protein Data Bank: architectural advances towards integrated searching and efficient access to macromolecular structure data from the PDB archive. *Journal of molecular biology*, *433*(11), p.166704.

[41]. Jejurikar, B.L. and Rohane, S.H., 2021. Drug designing in discovery studio.

[42]. Dallakyan, S. and Olson, A.J., 2015. Small-molecule library screening by docking with PyRx. *Chemical biology: methods and protocols*, pp.243-250.

[43]. Mooers, B.H., 2020. Shortcuts for faster image creation in PyMOL. *Protein Science*, *29*(1), pp.268-276.